Airflow-directed in situ electrospinning of a medical glue of cyanoacrylate for rapid hemostasis in liver resection

Article *in* Nanoscale · May 2014

DOI: 10.1039/c4nr01412j · Source: PubMed

7 authors, including:

Yun-Ze Long
Qingdao University
237 PUBLICATIONS **4,261** CITATIONS

SEE PROFILE

Xingyu Jiang
Southern University of Science and Technology
348 PUBLICATIONS **14,428** CITATIONS

SEE PROFILE

Nanoscale

COMMUNICATION

Airflow-directed *in situ* electrospinning of a medical glue of cyanoacrylate for rapid hemostasis in liver resection†

Cite this: *Nanoscale*, 2014, **6**, 7792

Received 14th March 2014
Accepted 14th April 2014

DOI: 10.1039/c4nr01412j

www.rsc.org/nanoscale

Kai Jiang,‡*[a] Yun-Ze Long,‡*[bc] Zhao-Jun Chen,[d] Shu-Liang Liu,[b] Yuan-Yuan Huang,[b] Xingyu Jiang[e] and Zhi-Qiang Huang[a]

Rapid hemostasis of solitary organs is still a big challenge in surgical procedures or after major trauma in both civilians and on the battlefield. Here, we report the first use of an airflow-directed *in situ* electrospinning method to precisely and homogeneously deposit a medical glue of *n*-octyl-2-cyanoacrylate (OCA) ultrathin fibers onto a wound surface to realize rapid hemostasis in dozens of seconds. *In vivo* and *in vitro* experiments on pig liver resection demonstrate that the self-assembled electrospun OCA membrane with high strength, good flexibility and integrity is very compact and no fluid seeping is observed even under a pressure of 147 mm Hg. A similar effect has been achieved in an *in vivo* experiment on pig lung resection. The results provide a very promising alternative for rapid hemostasis of solitary organs as well as other traumas, providing evidence that the postoperative drainage tube may not be always necessary for surgery in the near future.

Introduction

Rapid hemostasis of solitary organs is still a big challenge in surgical procedures and after major trauma especially in civilians and on the battlefield, because till now, only a few effective methods have been used to stop bleeding without causing secondary damage.[1] Present methods to control bleeding utilize hemostatic agents that include mechanical methods, thermal devices for cauterization, and vasoconstrictor chemicals. Among them, mechanical methods use pressure or ligature to slow the blood flow. Thermal devices commonly involve cauterization using electrodes, lasers, or heat. Chemical agents are those that can change the clotting activity of the blood or act as vasoconstrictors. All of them have their obvious different advantages and limitations. For example, fibrin products have been popularly used for many surgical procedures because of their biocompatibility, but the fibrin adhesive may activate an adverse immune response along with some other drawbacks such as low shelf-life, high expense, contamination with viruses or prions and relatively low bonding strength with load-carrying and flexible body parts.[2,3] Chitosan bandages are arguably the most promising for the hemostatic dressings and have been adopted by the US Department of Defense. However, the mechanism of the chitosan bandage interaction is not entirely understood, and the bandage seems to be not suitable for complex wounds.[3]

Since many of the currently used hemostats are difficult to be used in uncontrolled environments, as an alternative way, self-assembled materials to control bleeding, including self-assembling peptides,[4,5] hydrophobically modified chitosan,[6] and cyanoacrylates,[7–10] have been exploited in recent years. For example, researchers were amazed to see that self-assembled peptide fibers could immediately stop bleeding at the surgical site, which were originally designed to form an extracellular matrix to facilitate neuronal regeneration.[4,5] Ryu *et al.*[6] found that the blend mixture of the catechol-conjugated chitosan and the thiolated Pluronic F-127 remained at a viscous solution state at room temperature while it became a cross-linked gel state with instantaneous solidification at the body temperature and physiological pH, showing superior hemostatic properties.

Cyanoacrylates (CAs) have also been used widely for wound repair, hemostasis, and various surgical applications[10] since Coover *et al.*[11] reported on their applicability to wound closure in 1959. Now, 2-butyl cyanoacrylate (BCA) and 2-octyl cyanoacrylate (OCA) with improvement in strength and flexibility[12] have been granted approval by the US Food and Drug Administration

[a]*Institute & Hospital of Hepatobiliary Surgery, Key Laboratory of Digital Hepatobiliary Surgery of Chinese PLA, Chinese PLA Medical Academy, Chinese PLA General Hospital, Beijing 100853, P. R. China. E-mail: jiangk301@126.com*

[b]*College of Physics, Qingdao University, Qingdao 266071, P. R. China. E-mail: yunze.long@163.com*

[c]*Collaborative Innovation Center for Marine Biomass Fibers, Materials & Textiles of Shandong Province, State Key Laboratory Cultivation Base of New Fiber Materials & Modern Textile, Qingdao University, Qingdao 266071, P. R. China*

[d]*College of Chemical Engineering, China University of Petroleum (East China), Qingdao 266555, P. R. China*

[e]*Laboratory for Biological Effects of Nanomaterials & Nanosafety, National Center for Nanoscience & Technology, Beijing 100190, P. R. China*

† Electronic supplementary information (ESI) available. See DOI: 10.1039/c4nr01412j

‡ These two authors contributed equally to this work.

(FDA) for their use in man. Their advantages include the reduction in time required for wound closure, decreased pain scores, low expense compared to other tissue sealants and adhesives, and equivalent cosmetic outcomes. Although the long-term efficacy of OCA and BCA is still arguable,[10] there is a significant literature with respect to using cyanoacrylates for esophageal and gastric varices,[8,9,13–15] and clinical trials of internally usable cyanoacrylates have been performed.[16,17] For instance, animal studies have confirmed that OCA does not interfere with wound healing, has minimal toxicity[18] and may reduce the incidence of wound infection.

However, the application effect of cyanoacrylates and fibrin products is strongly limited by inhomogeneous and discontinuous coating by a conventional depositing way such as injection or daub, especially for large-area complex wounds. In addition, spraying can improve the coating homogeneity of cyanoacrylates or fibrin adhesives, for example, sprayed onto second-degree burns,[19] but it cannot precisely control the deposition range at wound sites, which may result in serious tissue adhesion especially in the abdominal cavity.

Electrospinning is a simple, highly versatile and effective nanotechnology to produce ultrathin polymeric and inorganic fibers with diameters down to a few nanometers and of a broad range of complex architectures and assemblies of nanofibers.[20,21] Typically, electrospinning apparatus consists of three elements: a high voltage power supply, a syringe with a spinneret, and a collector. The principle of electrospinning is straightforward: the polymer solution is first extruded from the spinneret to form a charged jet in the presence of a high-voltage electric field, and then the polymer jet undergoes straight fluid extension and followed vigorous whipping and/or splitting motion due to fluid and electrically driven bending instabilities; finally, the continuous ultrafine fibers are deposited on the collector in the form of a nonwoven web. Electrospun nanofibers from synthetic and natural biomedical polymers have a broad range of applications such as tissue engineering scaffolding, cosmetic skin mask, drug and/or gene delivery carrier, wound dressing, hemostatic devices, *etc.*[22–26]

In this article, we report on a modified electrospinning technique, namely, airflow-directed *in situ* electrospinning, which can precisely control the deposition of ultrathin polymeric fibers onto wound sites, and the first use of this technology on *in vitro* and *in vivo* experiments of rapid hemostasis in pig liver resection. Compared with other approaches, this technique can clean up the wounds first and then very rapidly, precisely deposit nanostructured hemostats on complex, irregular, large area wounds to form a continuous, compact, flexible membrane with excellent integrity, which acts as a powerful barrier to stop bleeding immediately and prevent possible blood or bile seeping.

Experiments and methods

Materials

508 medical glue (*Otologic and Craniocerebral Glue* series), mainly composed of *N*-octyl-2-cyanoacrylate (OCA) and a little medical PMMA as an additive, was purchased from Guangzhou Baiyun Medical Adhesive Co., Ltd, China and used directly without other treatments.

Airflow-directed *in situ* electrospinning setup

As shown in Fig. 1, the airflow-directed *in situ* electrospinning device mainly consists of four elements: a high-voltage power supply, a syringe pump, an air pump, and a home-made handle with a spinneret head. The positive electrode of the power supply (DW-P303-1ACFO, Tianjin Dongwen, China) is connected to the spinneret head to provide a high voltage of about 6–10 kV, which is necessary to generate electrospun fibers. A syringe is also connected to the spinneret and pushed by the syringe pump (LSP02-1B, Longer Pump, China) to provide a stable and appropriate feed rate (0.831 nl min^{-1} to 150.5 mL min^{-1}). In order to assist electrospinning and control the fiber deposition range, an air pump is connected to the home-made handle and spinneret head, which has a coaxial structure. The airflow also can be used to clean wounds before electrospinning, and its appropriate velocity was about 12 L min^{-1}.

In vitro and *in vivo* hemostasis experiments

In vitro experiments were carried out on fresh pig livers and lungs purchased from the market to study the directed deposition function of the home-made device and the physical properties of the electrospun OCA film. *In vivo* hemostasis experiments were carried out in 20 liver lobes of pigs (~40 kg, China landrace) obtained from the Chinese PLA General Hospital (Beijing). The surgical procedure was recorded by a digital camera. All the studies follow the Animal Ethics Committee rule and were approved by the Animal Ethics Committee of the Chinese PLA General Hospital.

Sample characterization

The electrospun OCA nanostructures were characterized by a Fourier transform infrared (FTIR) spectrometer (Thermo Scientific Nicolet iN10), an optical microscope (Olympus BX51), and a scanning electron microscope (SEM, Hitachi TM-1000). The cross-section of the pig liver covered by the electrospun OCA nanostructures was also characterized by SEM.

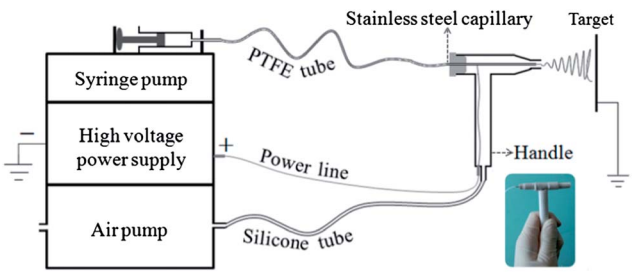

Fig. 1 Schematic illustration of the airflow-directed *in situ* electrospinning device. The inset is a camera picture showing the home-made handle and spinning head. This device design has been authored by China patent (ZL 2013 2 0741232.3).

Results and discussions

Electrospinning OCA ultrafine fibers and precise deposition

Different from the conventional electrospinning and spraying methods, one interesting feature of our home-made airflow-directed *in situ* electrospinning device is precise deposition on a desired site, namely, the deposition range and deposition position can be precisely controlled under the assistance of airflow. Two experiments demonstrate this function. In the first experiment, as shown in Fig. 2a–c, a culture dish with water was used as a collector. A small drop of red ink was added into the water to assist clear observation. Before electrospinning, the air pump was turned on, then the airflow could blow away the water and a small hole thus formed, indicating that the airflow can not only precisely direct electrospinning and deposition, but also help to clean the collector surface (or the wound surface). When a high voltage was applied, the electrospun OCA fibers were deposited and polymerized rapidly on the hole surface to form a solid self-assembled membrane. After electrospinning stops, the hole could be kept due to the self-assembled OCA film. In another experiment, as shown in Fig. 2d and ESI Video 1,† the airflow-directed *in situ* electrospinning device with precise deposition function could be used as a pen to write words such as "electrospinning". The inset optical microscopic image shows that the letter was composed of electrospun OCA fibers. It is noted that the deposition width increases gradually with the increase of electrospinning height, as shown in Fig. 3. When the spinning head-to-collector distance is 4–5 cm (present case), the deposition width is about 8 mm.

There are several parameters that can affect the morphology and structure of electrospun fibers. The optimized conditions for well assembled OCA ultrathin fibers are: applied voltage 9 kV, nozzle tip-to-collector distance 5–6 cm, airflow velocity 12 L min^{-1}, solution feed rate 30 μL min^{-1} (Fig. 2e) and electrospinning time of 2 s. When the feed rate was larger than 150 μL min^{-1}, the electrospun structures became beaded fibers and beads gradually (Fig. 2f). In order to prove that the OCA monomer was polymerized into poly(*n*-octyl-2-cyanoacrylate) (POCA) in the fibers, the as-spun samples were characterized by FTIR spectroscopy (Fig. 4). The presence of C≡N stretching mode in the spectrum demonstrates the existence of POCA in the electrospun fibers (Table 1).[27] The fiber solidification mechanism during the electrospinning process could be ascribed to the rapid polymerization (self-assembly) of the OCA monomer in the presence of water (anionic initiator), forming long, strong chains. The electrospun OCA fibers also can be formed directly on the liver surface when using a pig liver as collector. Fig. 2g and h show the surface morphology and cross-sectional structure of the electrospun OCA coating on the pig liver, respectively, fabricated under conditions of a feed rate of 30 μL min^{-1} and an electrospinning time of 20 s. The self-assembled OCA nanostructures formed a very compact membrane and barrier bonding with the pig liver.

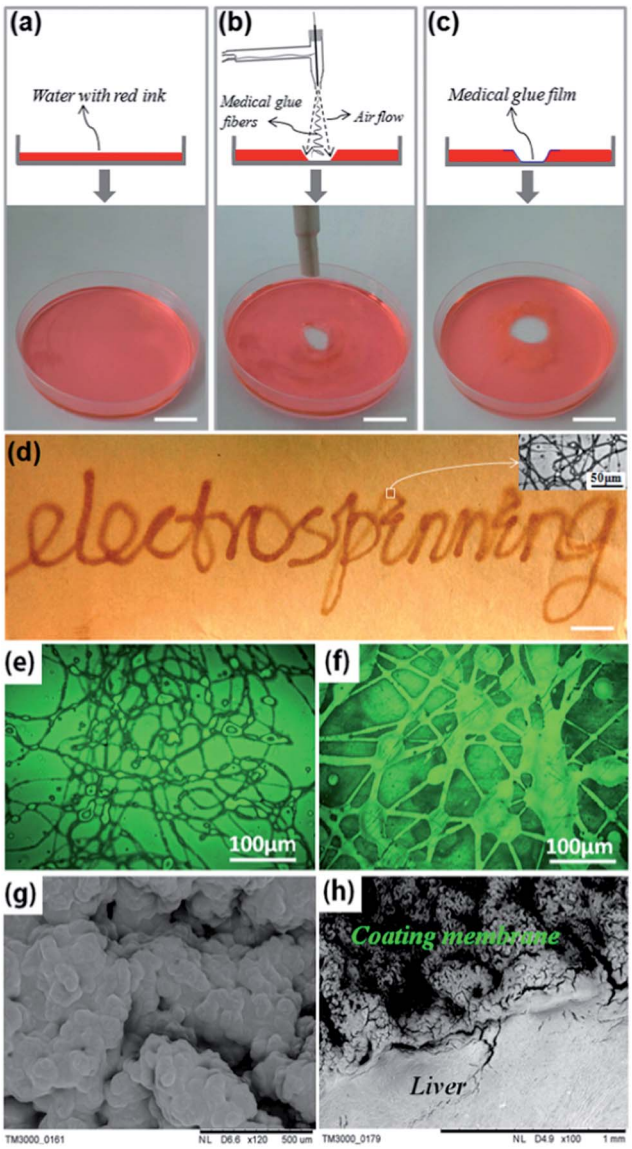

Fig. 2 (a–d) Precise deposition of medical glue OCA fibers *via* the airflow-directed *in situ* electrospinning technique. (a) A culture dish with red water. (b) The airflow could blow away the water and form a small hole, then electrospun OCA fibers were deposited on the surface to form a self-assembled membrane. (c) The hole could be kept after removing the spinning handle. (d) This setup could be used as a pen to write, please see ESI Video 1.† The inset is an optical image. The scale bar in (a–d) is 20 mm. (e–f) Optical images of OCA fibers fabricated under conditions of applied voltage 9 kV, nozzle tip-to-collector distance 4–5 cm, airflow velocity 12 L min^{-1}, solution feed rate 30 μL min^{-1} (e) or 150 μL min^{-1} (f), and spinning time 2 s. The electrospun structures became beaded fibers and beads when the feed rate was larger than 150 μL min^{-1}. (g–h) SEM images of the electrospun OCA coating on the pig liver (30 μL min^{-1} and 20 s). (g) Surface morphology and structure. (h) Cross-sectional view, indicating a strong combination of the self-assembled OCA membrane with the pig liver.

Rapid coating complex large-area liver wounds

Besides small wounds and cuts, the airflow-directed *in situ* electrospinning device is particularly suitable for rapid coating of a self-assembled OCA membrane on complex, large-area

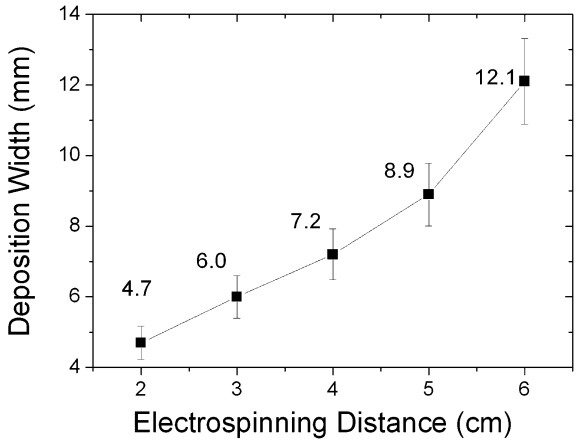

Fig. 3 The relationship between the electrospinning height and the width of the OCA fiber line that was deposited on the collector under conditions of applied voltage 9 kV, airflow velocity 12 L min^{-1}, solution feed rate 150 μL min^{-1}. With the assistance of the airflow, the OCA fibers can deposit on the collector precisely. Usually, an electrospinning height of 3–5 cm is used according to the practical need.

wounds in 1–2 minutes. Three kinds of complex large-area wounds of pig livers have been used for demonstration: section wound with a width of 6–7 cm and a height of 2–3 cm after resection (Fig. S1a†) and trench-like wounds with an area of 2.5 × 2.5 cm^2 and a depth of 0.5 cm (Fig. S1b and c†). For the section wound after resection, the artery blood vessel was blocked by a small piece of gelatin sponge (white color, marked by a red arrow) to stop bleeding before electrospinning. As shown in Fig. S1d and e and the ESI Video,† these liver wounds can be covered by a layer of OCA fiber film very precisely and rapidly in 100 s using the airflow-directed *in situ* electrospinning device, indicating that a new continuous membrane with excellent integrity is reconstructed to protect the wound.

Table 1 Major mid-IR peak assignments for the cyanoacrylate system

Wave numbers (cm^{-1})	Peak assignments and comments
3447.82	–O–H stretching vibration
3080–2800	C–H stretching vibrations (symmetric and asymmetric) of $-CH_2-$ and CH_3- groups
2247.72	–C≡N stretching vibration
1751.31	–C=O stretching vibration
1500–400	CH_2 and CH_3 scissoring and bending region

Strength and compactness of the electrospun membrane

We first show the bonding toughness of the as-formed nanofibrous membranes. It has been reported that the films made up of OCA and BCA glues have high strength and strong tissue bonding ability.[28] In this article, we also tested the strength, compactness and integrity of the electrospun membrane. As shown in Fig. S2,† the liver wound was covered by a piece of surgical gauge, and then a layer of electrospun OCA was deposited on it. Several minutes later, the pig liver (~0.5 kg) could be hanged by hooking the surgical gauge, indicating that the surgical gauge was fixed on the liver surface very strongly using the electrospun OCA coating. This coating with good flexibility and high strength could not be peeled off from the liver even if a force larger than 30 N was applied. The strong bonding with tissue could be ascribed to the self-assembled OCA film (Fig. S2c†), which fixed the surgical gauge to the liver surface toughly.

We next show that the electrospun membrane would withstand high pressure. To do so, (a) a two-meter-high pipe was connected to the hepatic artery of a fresh pig liver (Fig. S3a†). (b) Part of the liver was cut. Fig. S3b† shows the cross-section of the liver and the artery blood vessel can be seen obviously. (c) Before

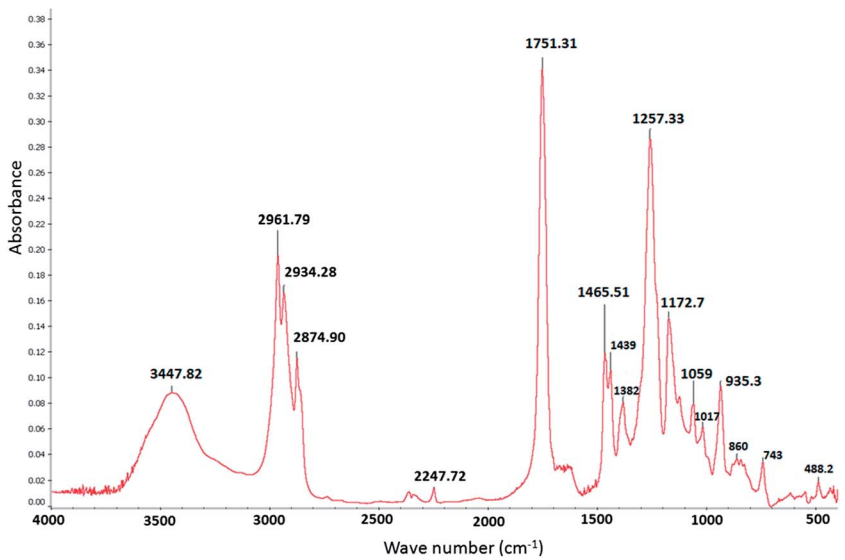

Fig. 4 Fourier transform infrared (FTIR) spectra of the electrospun medical glue membrane (Thermo Scientific Nicolet iN10). Mid-IR peak assignments of the cyanoacrylate system are presented in Table 1.

coating OCA glue, the artery blood vessel was blocked by a small piece of gelatin sponge, then the entire wound was coated by a layer of OCA fiber membrane *via* the airflow-directed *in situ* electrospinning device, and then the two-meter high pipe was filled with water. It was surprising to see that no blood/water leakage was observed for 12 h under the two-meter-high hydraulic pressure (~147 mm Hg), indicating very high compactness and strength of the electrospun OCA fiber membrane. A further experiment also showed that as high as 2.65-meter-high hydraulic pressure (~195 mm Hg) could be applied on the liver wound without water seeping.

Besides pig liver, an *in vitro* experiment was also performed on a fresh pig lung to test the leak proofness of the electrospun OCA membrane. As shown in Fig. S4 and ESI Video 2,† firstly, part of the lung was cut, and air leakage (air bubbles on the wound) could be observed clearly when air was pumped into the lung (12 L min^{-1}, 2 kPa) and water was dropped onto the wound. Secondly, before electrospinning, the bronchi were blocked by a small piece of gelatin sponge (marked by an arrow), then the entire wound was coated by a layer of OCA fiber membrane *via* the airflow-directed *in situ* electrospinning device. Finally, when air was pumped into the lung (12 L min^{-1}, 2 kPa) and water was dropped on the wound, no air seeping (air bubble) was observed, indicating perfect leak proofness of the electrospun OCA membrane. ESI Video 2† exhibits this experimental result (air leakage on the wound before electrospinning and no air seeping after membrane deposition) clearly.

In vivo rapid hemostasis in pig liver resection

In order to further verify the validness of this technology, an *in vivo* hemostasis experiment in a pig model has also been carried out. Fig. 5a shows the schematic illustration of the experimental procedure. Camera images at each stage of the *in vivo* hemostasis experiment on pig liver are shown in Fig. 5b–h and ESI Video 3.† Firstly, a piece of liver was exposed from the abdominal cavity of a pig under anesthesia, and fixed by a pair of hemostatic forceps. Secondly, part of the liver was cut, and wound weeping could be seen obviously. Thirdly, the blood was cleaned by a sterile gauze and further cleaned by the airflow, and then the wound was rapidly covered by a layer of OCA fiber film using the airflow-directed *in situ* electrospinning device in

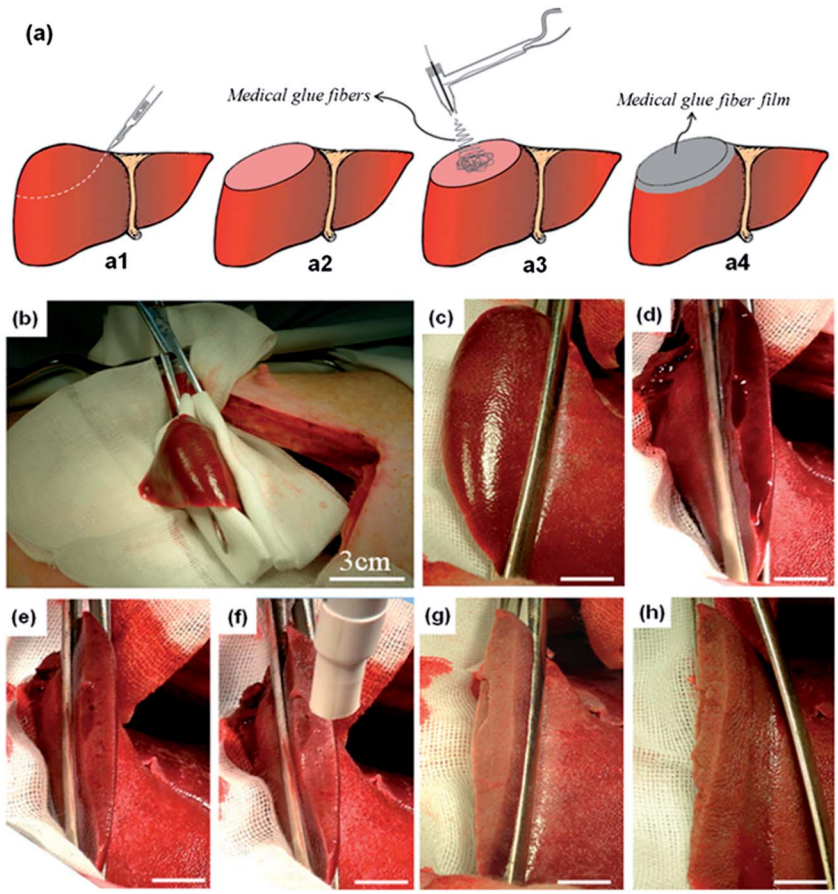

Fig. 5 Complete *in vivo* pig liver hemostasis. (a) Schematic illustration of the experimental procedure. (b–h) The pictures are time-lapse camera images at each stage of the *in vivo* hemostasis experiment for wound section in pig liver. (b) A piece of liver was exposed from the abdominal cavity of a pig under anesthesia. (c) The liver was fixed by a pair of hemostatic forceps. (d) Part of the liver was cut and the wound was weeping. (e) The blood was cleaned by the sterile gauze or airflow. (f) The wound was further cleaned by the airflow. (g) The wound was then rapidly covered by a layer of OCA fiber film using airflow-directed *in situ* electrospinning in 20 s. (h) No blood or bile seeping was observed after removing the hemostatic forceps. The scale bar in (c–h) is 10 mm. The complete process is demonstrated clearly in ESI Video 3.†

20 s. One minute later, the hemostatic forceps were removed, no blood seeping was observed for the following 3 hours. It is noted that during this liver resection procedure, no other hemostats and sealants were used. Particularly, *in vivo* hemostasis experiments have been carried out in pigs for more than 20 times, and similar results have been obtained, indicating excellent repeatability and reliability of this technology.

As mentioned above, during electrospinning, the OCA monomer is exposed to anionic initiators such as water molecules (hydroxyl groups or lone pairs of electrons on pendant NH_2 groups) on the wound surfaces, inducing polymerization to form long, strong chains. The nanostructured OCA membrane can strongly adhere onto the surrounding tissue and be rapidly solidified to serve as a protective barrier to stem the flow of blood and facilitate the movement of adjacent cells to repair the injured site.[4–6,29] Luo *et al.* proposed that the dense self-assembling peptide nanofiber scaffold resembles the multi-layered fish-net, and thus prevents escape of the cells and fluid.[5] So, in this case, keeping the continuity and integrity of the covered membrane becomes significant especially for large-area and irregular shapes of the wounds, which can be achieved easily by the airflow-directed *in situ* electrospinning technology.

Conclusions

The goal of this work is to find a cost-effective method to quickly stop bleeding and protect wounds with large area and irregular shapes in clinical surgery such as liver or lung resection. To achieve this goal, we design an airflow-directed *in situ* electrospinning device, and take FDA-approved OCA medical glue as an example to test its effect. Experimental results indicate that this technology can reconstruct a nanostructured coating very quickly on complex wounds. In particular, this self-assembled membrane exhibits excellent continuity, integrity, flexibility, compactness and high strength, and can bear a two-meter high hydraulic pressure (~147 mm Hg) without fluid seeping. This nanotechnology may be very promising in surgery especially on solitary organs to reduce surgery time, lower medical cost and enhance operation safety without using some traditional agents/methods to stop bleeding in operation and without using a drainage tube after operation. However, the practicability of this technology needs more and further studies and the applicability of other agents such as fibrin products should be tested. Such work is in progress.

Conflict of interest

The authors declare no competing financial interest.

Acknowledgements

This work was supported by the National Natural Science Foundation of China (51373082), National Key Technology R&D Program of China (2012BI06B01), Natural Science Foundation of Shandong Province, China, for Distinguished Young Scholars (JQ201103), Taishan Scholars Program of Shandong Province (ts20120528), National Key Basic Research Development Program of China (973 special preliminary study plan, 2012CB722705), and Program for Scientific Research Innovation Team in Colleges and Universities of Shandong Province, China.

References

1 L. Ivanciu, R. Toso, P. Margaritis, G. Pavani, H. Kim, A. Schlachterman, J. H. Liu, V. Clerin, D. D. Pittman, R. Rose-Miranda, K. M. Shields, D. V. Erbe, J. F. Tobin, V. R. Arruda and R. M. Camire, *Nat. Biotechnol.*, 2011, **29**, 1028.
2 K. King, M. C. Neuffer, J. McDivitt, D. Rose, C. C. Cloonan and J. S. Vayer, *Mil. Med.*, 2004, **169**, 716.
3 H. B. Alam, D. Burris, J. A. DaCorta and P. Rhee, *Mil. Med.*, 2005, **170**, 63.
4 R. G. Ellis-Behnke, Y. X. Liang, D. K. C. Tay, P. W. F. Kau, G. E. Schneider, S. G. Zhang, W. T. Wu and K. F. So, *Nanomedicine*, 2006, **2**, 207.
5 Z. L. Luo, S. K. Wang and S. G. Zhang, *Biomaterials*, 2011, **32**, 2013.
6 J. H. Ryu, Y. Lee, W. H. Kong, T. G. Kim, T. G. Park and H. Lee, *Biomacromolecules*, 2011, **12**, 2653.
7 B. Petersen, A. Barkun, S. Carpenter, P. Chotiprasidhi, R. Chuttani, W. Silverman, N. Hussain, J. Liu, G. Taitelbaum and G. G. Ginsberg, *Gastrointest. Endosc.*, 2004, **60**, 327.
8 Y. T. Lee, F. K. L. Chan, E. K. W. Ng, V. K. S. Leung, K. B. Law, M. Y. Yung, S. Chung and J. J. Y. Sung, *Gastrointest. Endosc.*, 2000, **52**, 168.
9 Y. H. Huang, H. Z. Yeh, G. H. Chen, C. S. Chang, C. Y. Wu, S. K. Poon, H. C. Lien and S. S. Yang, *Gastrointest. Endosc.*, 2000, **52**, 160.
10 K. P. Davis and R. W. Derlet, *Wild. Environ.Med.*, 2013, **24**, 67.
11 H. W. Coover, F. B. Joyner, N. H. Shearer and T. H. Wicker, *J. Soc. Plast. Surg. Eng.*, 1959, **15**, 413.
12 A. J. Shapiro, R. C. Dinsmore and J. H. North, Jr, *Am. Surg.*, 2001, **67**, 1113.
13 B. D. Greenwald, S. H. Caldwell, E. E. Hespenheide, J. T. Patrie, J. Williams, K. F. Binmoeller, L. Woodall and O. Haluszka, *Am. J. Gastroenterol.*, 2003, **98**, 1982.
14 C. J. Chang, M. C. Hou, H. C. Lin, H. S. Lee, W. C. Liao, C. W. Su and S. D. Lee, *Gastrointest. Endosc.*, 2010, **71**, 1141.
15 S. Seewald, T. L. Ang, H. Imazu, M. Naga, S. Omar, S. Groth, U. Seitz, Y. Zhong, F. Thonke and N. Soehendra, *Gastrointest. Endosc.*, 2008, **68**, 447.
16 W. G. Schenk, W. D. Spotnitz, S. G. Burks, P. H. Lin, R. L. Bush and A. B. Lumsden, *Am. Surg.*, 2005, **71**, 658.
17 A. B. Lumsden and E. R. Heyman, *J. Vasc. Surg.*, 2006, **44**, 1002.
18 D. M. Toriumi, W. F. Raslan, M. Friedman and M. E. Tardy, Jr, *Laryngoscope*, 1991, **101**, 339.
19 A. J. Singer, M. Mohammad, H. C. Thode, Jr and S. A. McClain, *Burns*, 2000, **26**, 388.
20 D. H. Reneker and A. L. Yarin, *Polymer*, 2008, **49**, 2387.
21 S. Agarwal, A. Greiner and H. Wendorff, *Prog. Polym. Sci.*, 2013, **38**, 963.

22 T. Dvir, B. P. Timko, D. S. Kohane and R. Langer, *Nat. Nanotechnol.*, 2011, **6**, 13.
23 S. Agarwal, J. H. Wendorff and A. Greiner, *Adv. Mater.*, 2009, **21**, 3343.
24 D. Kai, G. Jin, M. P. Prabhakaran and S. Ramakrishna, *Biotechnol. J.*, 2013, **8**, 59.
25 M. M. Li, W. W. Liu, J. S. Sun, Y. L. Xianyu, J. D. Wang, W. Zhang, W. F. Zheng, D. Y. Huang, S. Y. Di, Y. Z. Long and X. Y. Jiang, *ACS Appl. Mater. Interfaces*, 2013, **5**, 5921.
26 B. Sun, Y. Z. Long, H. D. Zhang, M. M. Li, J. L. Duvail, X. Y. Jiang and H. L. Yin, *Prog. Polym. Sci.*, 2013, **39**, 862.
27 S. K. Tomlinson, O. R. Ghita, R. M. Hooper and K. E. Evans, *Vib. Spectrosc.*, 2006, **40**, 133.
28 L. C. Perry, *An evaluation of acute incisional strength with traumaseal surgical tissue adhesive wound closure*, Dimensional Analysis Systems Inc, Leonia, NJ, 1995.
29 M. Levi, P. W. Friederich, S. Middleton, P. G. de Groot, Y. P. Wu, R. Harris, B. J. Biemond, H. F. G. Heijnen, J. Levin and J. W. ten Cate, *Nat. Med.*, 1999, **5**, 107.